Dalton Transactions

PERSPECTIVE

View Article Online
View Journal

Cite this: DOI: 10.1039/c4dt03013c

Synthesis methods to prepare single- and multi-core iron oxide nanoparticles for biomedical applications†

L. Gutiérrez,*[a] R. Costo,[a] C. Grüttner,[b] F. Westphal,[b] N. Gehrke,[c] D. Heinke,[c] A. Fornara,[d] Q. A. Pankhurst,[e] C. Johansson,[f] S. Veintemillas-Verdaguer[a] and M. P. Morales*[a]

Received 30th September 2014,
Accepted 20th December 2014

DOI: 10.1039/c4dt03013c

www.rsc.org/dalton

We review current synthetic routes to magnetic iron oxide nanoparticles for biomedical applications. We classify the different approaches used depending on their ability to generate magnetic particles that are either single-core (containing only one magnetic core, *i.e.* a single domain nanocrystal) or multi-core (containing several magnetic cores, *i.e.* single domain nanocrystals). The synthesis of single-core magnetic nanoparticles requires the use of surfactants during the particle generation, and careful control of the particle coating to prevent aggregation. Special attention has to be paid to avoid the presence of any toxic reagents after the synthesis if biomedical applications are intended. Several approaches exist to obtain multi-core particles based on the coating of particle aggregates; nevertheless, the production of multi-core particles with good control of the number of magnetic cores per particle, and of the degree of polydispersity of the core sizes, is still a difficult task. The control of the structure of the particles is of great relevance for biomedical applications as it has a major influence on the magnetic properties of the materials.

Introduction

The number of biomedical applications using magnetic iron oxide nanoparticles has been increasing exponentially over the past few years.[1,2] A few examples are: magnetic biosensor systems,[3] local heat sources for cancer treatment by hyperthermia,[4] separation immunoassays,[5] drug carriers,[6] contrast agents for magnetic resonance imaging[7] (MRI) and magnetic particle imaging (MPI),[8,9] parasite diagnostic assays,[10–12] and nanobridging substances for surgery and wound healing.[13]

In the absence of specific coatings, magnetic nanoparticles tend to form aggregates. *N.B.* For this reason, nomenclature can be problematic, with the term 'particle' being used to describe both an individual nanoparticle and a collection of them. In this review we will use the term 'core' to describe an individual nanoparticle, and 'multi-core' to describe a collection of cores held by a matrix forming a fixed structure. Our definition of single- and multi-core particles considers these materials as discrete identifiable entities that could further agglomerate, but, in this case, the agglomeration would always be a consequence of weak physical interactions in a reversible process. To differentiate this reversible agglomeration process from stronger irreversible processes, we have used the term "aggregate" to refer to the stronger assemblage that occurs in multi-core nanoparticles to generate the discrete entity.

The aggregation (and, in some cases, further agglomeration) state of the particles is of great relevance because the magnetic properties of these systems exhibit a dramatic change with variations on the magnetic interactions between cores and with the surrounding matrix.[14] In addition to the forces that may arise when nanoparticles, composed of any material, are dispersed in an inert liquid (*e.g.* Van der Waals or electrostatic forces), magnetic nanoparticles may also present magnetic forces between nanoparticles due to magnetic dipole–dipole interactions or exchange interactions if the particles are in close contact.[15] Dipolar interactions are relatively long range and their strength depends, among other factors such as particle size and shape, on the interparticle distance.[16] Therefore, when magnetic nanoparticles aggregate, or above a

[a]*Instituto de Ciencia de Materiales de Madrid, ICMM-CSIC, Cantoblanco, 28049 Madrid, Spain. E-mail: lucia@icmm.csic.es, puerto@icmm.csic.es*
[b]*Micromod Partikeltechnologie GmbH, D-18119 Rostock, Germany*
[c]*NanoPET Pharma GmbH, D-10115 Berlin, Germany*
[d]*SP Technical Research Institute of Sweden, Box 5607 SE-114 86 Stockholm, Sweden*
[e]*Institute of Biomedical Engineering, University College of London, London WC1E 6BT, UK*
[f]*Acreo Swedish ICT AB, Arvid Hedvalls Backe 4, Box 53071 SE-400 14 Göteborg, Sweden*

†Electronic supplementary information (ESI) available. See DOI: 10.1039/c4dt03013c

certain particle concentration, the dynamic and DC magnetic properties of magnetic nanoparticle systems are altered due to magnetic interactions,[17,18] significantly changing the properties of the material if compared to a non-interacting system. Although nanoparticle synthesis naturally leads to materials with different aggregation degrees, there has been little attention paid to which is better for what application. For example, multi-core particles seem to have superior performance for magnetic hyperthermia[19,20] or MPI, although this fact is strongly affected by the chain or column formation of the particles[21] within the applied magnetic field. In contrast, there is much discussion of the advantages of monodisperse single-core nanoparticles having uniform properties, for *e.g.* targeted delivery, since size determines its pharmacokinetic behaviour and therefore its biodistribution. The use of some materials for combined applications (targeting, diagnostics, and therapy) would also require a careful tuning of the particles properties.[22] Furthermore, there are some applications (*e.g.* sensors) in which it is essential to distinguish the cores' spontaneous agglomeration due to magnetic interactions from clustering induced by interactions with biomolecules or local pH changes. Therefore, specific protocols to obtain either single- or multi-core magnetic nanoparticles are required to match their magnetic properties with the requirements of each specific application, sometimes at the expense of their colloidal properties.

Producing single-core iron oxide nanoparticles is not an easy task. Ideally, these materials contain just one magnetic core per particle (Fig. 1). Nowadays, there are just few coating methods that can be used to prevent aggregation by minimizing the inter-particle interactions.

Magnetic multi-core nanoparticles are composed of several cores per particle (Fig. 1). In contrast with agglomerates of single-core particles, multi-core particles are assembled within a matrix that prevents further changes to the number of cores per particle with time. These systems may present strong magnetic interactions between the cores as a result of their close proximity to each other.[23] In this case, the number of magnetic cores per particle, their sizes, the distances between them, and their spatial distribution in general, will all strongly affect the magnetic properties of the material.

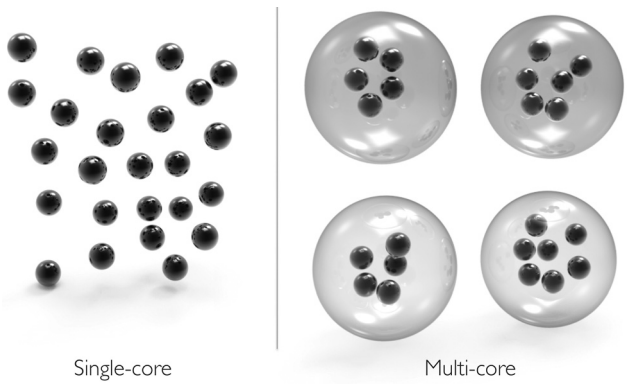

Fig. 1 Schematic representation of single-core and multi-core particles. Single-core particles contain only one magnetic core (single domain nanocrystal) per particle. Multi-core particles contain several magnetic cores per particle assembled within a matrix that prevents changes in the number of cores per particle with time.

The complexity of the problem of understanding the different magnetic properties of single-core and multi-core particles underlies the importance of reliable nanoparticle synthesis methods able to reproduce nanoparticle size, shape and structural homogeneity. Stable and reproducible analysis methods are also needed to characterize the different magnetic particle systems.

Although there are many other available magnetic materials, the most commonly used ones for biomedical applications are iron oxides, for the simple but profound reason that the human body has the organs and metabolic mechanisms to transfer iron into safe storage for later use.[24–26] Magnetite (Fe_3O_4) and maghemite (γ-Fe_2O_3) are the two main iron oxides being used as core materials of magnetic nanoparticles for biomedical applications. Unfortunately, distinguishing the exact crystalline structure of iron oxide nanoparticles, especially if mixed phases are present, is not an easy task[27] and, therefore, the structural information is not always available in the literature.

It should be noted that iron oxide nanoparticles as obtained directly after synthesis are not usually bio-tolerable *per se* and thus, should not normally be used directly for biomedical applications. Especially if the nanoparticles are intended for *in vivo* applications, several further steps are often necessary. For example, typical post-synthesis steps may involve the complete removal of any potentially toxic compounds remaining from the synthesis steps. The development of a suitable pharmaceutical formulation for the particles, including additives and excipients, to provide a sterile and iso-osmolar solution of bio-tolerable pH, containing only compounds suitable for the intended administration route (*e.g.* for intravenous injection), is similarly important.

Furthermore, *in vitro* toxicity tests should be performed prior to any *in vivo* application, and medium-term to long-term stability studies of the particles in the respective solutions should be conducted.[28] In case of *in vitro* applications the chosen solution has to be suitable for the *in vitro* assay (*e.g.* the respective cell line), as well as for the maintenance of colloidal stability. Although in contrast to human applications no approval by authorities is required for use of the particles for biomedical research purposes, it is recommended to perform those additional steps in order to obtain reliable, reproducible and significant results, as well as to comply with the ethic requirements for animal studies.

The object of this review paper is to describe a number of proven synthesis routes for magnetic nanoparticles intended for use in biomedical applications. Our aim is to go further than other magnetic nanoparticle synthesis reviews[29] by classifying the different routes depending on their capacity to produce single-core or multi-core nanoparticles that can be transferred in a carrier liquid for biomedical applications.

Single-core nanoparticles

Several chemical methods have been developed to synthesize magnetic nanoparticles, such as *via* microemulsions, sol–gel synthesis, hydrothermal reactions, hydrolysis and thermolysis of precursors, and other less common techniques.[30] We describe the most widely used synthesis routes below, classified depending on whether aqueous or organic phase precursors are used, and focusing on their capacity for the production of single-core particles.

Aggregation processes may occur during particle synthesis due to the large surface area of the nano-sized particles. Therefore, the use of surfactants to prevent particle aggregation is crucial for the attainment of single-core particles. However, many surfactants are toxic (*e.g.* Triton[31] or didodecyldimethylammonium bromide[32]), in which case they have to be removed or replaced by suitable ones prior to *in vivo* applications. In any post synthesis process, precautions have to be taken – the use of controlled microenvironments such as microemulsions for example – to avoid removing the primary surfactant and thereby reducing the stability of the product with regard to aggregation, agglomeration and precipitation.

Single-core nanoparticles from aqueous phase synthesis

Most of the single-core magnetic nanoparticles synthesis routes in aqueous phases are based on the Massart procedure, which produces iron oxide particles by alkaline precipitation of $FeCl_3$ and $FeCl_2$.[33] To reduce the polydispersity of the particles obtained, a size selection process is performed afterwards. Larger particles from the colloid are precipitated from the colloid by addition of an electrolyte solution or an antisolvent, leaving nearly monodisperse smaller particles in the supernatant. Particles are then coated to prevent aggregation. Single-core, non-aggregated particles have been obtained with sodium citrate, sodium polyacrylate or silica coatings leading to hydrodynamic particle diameters smaller than 20 nm. Coating methods are briefly summarized below.

Citrate coating. Iron oxide particles with a core diameter of around 5 nm have been coated with a citrate layer resulting in a hydrodynamic diameter of 8 nm.[34] Briefly, a mixture of ammonia water and citric acid are added to a mixture of $FeCl_3$ and $FeCl_2$ heated to 100 °C in the absence of oxygen. The solution is boiled for 10 min and then cooled down to room temperature.[35] R1 and R2 of these particles were 20.1 mM^{-1} s^{-1} and 37.1 mM^{-1} s^{-1} respectively,[36] suggesting their use as dynamic T1-weighted MRI contrast agents.[37] Among other examples, these particles have also been studied as contrast agents for magnetic resonance angiography in pigs.[38] Furthermore, they have been tested in clinical trials up to Phase I.[39]

Polyacrylate coating. This method produces hydrodynamic sizes of the coated magnetic nanoparticles 5 nm larger than the uncoated particles.[40,41] Poly(sodium acrylate), (either M_w = 2000 g mol^{-1} or 5000 g mol^{-1}) is added to the iron oxide suspension at pH 2, resulting in a precipitate that is then separated by centrifugation. Afterwards, the pH is increased up to 7–8 until the particles are redispersed spontaneously. These samples have been used to generate a model to predict the efficiency of magnetic nanoparticles as T2 MRI contrast agents.[41]

Silica coating. This type of coating is performed by modifications of the Stöber method that was originally described to prepare monodisperse silica particles in 1968.[42] The Stöber method is based on the hydrolysis of TEOS (Tetraethyl orthosilicate) in alcoholic solutions. This method is fast and very simple; however, it has several drawbacks, for instance, the secondary nucleation of silica particles, the difficult control of the silica shell thickness and the problems of coating particles individually.

A better control of the silica coating can be achieved by hydrolysis of TEOS in a microemulsion.[43,44] In this method, the size of the particles is limited by the size of the water droplets. Briefly, for this procedure, two separate inverse microemulsions have to be prepared using a surfactant (*e.g.* Brij-97 or Igepal CO-520). The first microemulsion contains $FeSO_4$ and $FeCl_3$, while the second microemulsion contains a base, either NaOH or NH_4OH, and neat TEOS. After stirring, the second microemulsion is added dropwise to the first one, placed in an ultrasonic bath. The reactants are mixed when the water droplets collide, producing the nanoparticles. The hydrolysis of TEOS catalyzed by the base produces silicic acid, which polymerizes forming the silica coating.[43]

Deposition of silica from silicic acid solutions and subsequent treatment with sodium silicate[45,46] can also be used to coat the particles with silica, although in this case, the control of the thickness of the silica layer below 50 nm is still difficult. The relevance of this coating for biomedical applications is due to the strong effect of the silica coating thickness on the relaxivity properties of these particles in aqueous suspensions.[46]

Single-core nanoparticles from organic phase synthesis

Two different organic phase approaches are commonly used: the thermal decomposition of organometallic compounds, and the polyol method.

Thermal decomposition of organometallic compounds. Thermal decomposition of organometallic compounds is able to produce magnetic nanoparticles with good crystallinity and high monodispersity, albeit usually with hydrophobic properties.[47] This approach offers two routes to very good control of the nucleation and growth processes that occur during the particles synthesis. One procedure is the injection of organometallic compounds into a hot surfactant solution, which results in the formation of nuclei almost instantaneously. The other option is the controlled heating of organometallic compounds in a surfactant solution to generate the nuclei. Once the nucleation has occurred, particles grow at high temperature. Finally, through a quick decrease of the reaction temperature, the growth of the nanoparticles can be stopped.

Single-core iron oxide nanocubes with sizes in the range between 20 nm and 160 nm have been synthetized with iron acetylacetonate in oleic acid and benzyl ether.[48] Alternative iron precursors include iron oleate[49] and iron pentacarbonyl.[50]

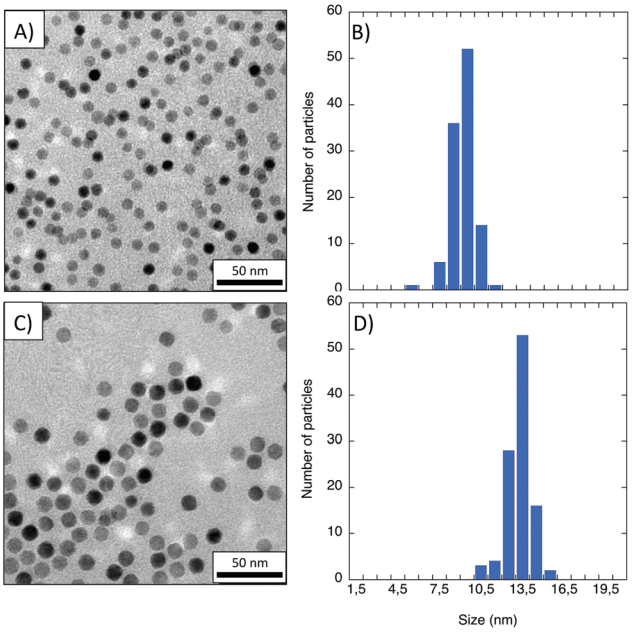

Fig. 2 TEM pictures and core size histograms of two different single-core nanoparticles prepared by thermal decomposition of organometallic compounds, prepared following the protocol described by Salas *et al.*[54]

Particle size can be controlled by varying the precursor concentration, the Fe/oleic acid ratio[51] or the solvents used.[49,52] Particle shape may be modified from spheres to cubes by adding sodium oleate to the synthesis.[53] Two examples of particles obtained by thermal decomposition of organometallic compounds showing very narrow core size distributions can be observed in Fig. 2.

The major drawback of organic phases syntheses is the additional step needed, after the synthesis, to stabilize the particles in aqueous medium, for use in biomedical applications. This transfer to water can lead to irreversible aggregation of the particles. Below, we summarize the most common methods that are employed that avoid this outcome, and that can successfully transfer particles from non-polar solvents to aqueous media in the form of individual particles.

Ligand exchange. The exchange of surface-coating oleic acid ligand molecules by dimercaptosuccinic acid (DMSA) molecules leads to highly negatively charged surfaces and hydrodynamic sizes smaller than 50 nm, even for core sizes up to 22 nm.[54] DMSA also provides free ligand groups for biomolecule conjugation. Briefly, a dispersion of particles in toluene is mixed with a solution of DMSA in dimethylsulfoxide (DMSO) and stirred mechanically for several hours to allow the ligand exchange. After that, the particles are washed several times to remove any organic waste and are then redispersed in water. Particles obtained by this procedure have been successfully used as drug delivery systems.[6]

Silica coating by inverse microemulsion. This process has shown very good results in terms of keeping particles permanently apart. Organic-soluble nanoparticles are transferred to water-soluble condition by adding a silica layer with thickness between 1 and 50 nm.[55–57] Several protocols can be followed to perform the silica coating by this procedure, although some of them, including products such as Triton, are not recommendable at all if biomedical applications are intended. One suitable option is to suspend particles in cyclohexane and mixed them with a solution of Igepal CO520 and cyclohexane. A stable inverse microemulsion is then obtained by adding NH_4OH. Then, the addition of TEOS to the solution results in its hydrolysis and subsequent condensation reaction generates the silica layer. Among other parameters, narrow size distributions and an ultrathin silica layer can be obtained by tuning the iron oxide concentration. It is even possible to coat iron oxide nanoparticles with a layer of mesoporous silica to allow the loading and release of active compounds or improve their performance as MRI contrast agents.[58] Changes on the experimental conditions of the protocol described for the silica coated single-core particles may lead to multi-core particles (Fig. 3).

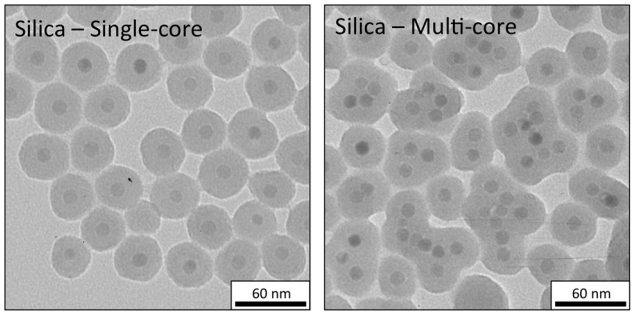

Fig. 3 TEM pictures showing single- (left) and multi-core (right) silica coated particles prepared by microemulsions (prepared with a protocol similar to the one described by Lee *et al.*[59]) using magnetic cores prepared by thermal decomposition of organometallic compounds.

Addition of an amphiphilic polymer. In this method the hydrophobic tails of the amphiphilic polymer intercalate the hydrophobic surfactant molecules present on the particle surfaces. The hydrophilic backbone of the polymer is exposed to the environment, leading to particle solubility in water. This approach results in hydrodynamic sizes of the particles about 8–10 nm larger than their inorganic core size measured by TEM.[60] A simple inexpensive and scalable production process is based on the use of an amphiphilic polymer made of poly (maleic anhydride) modified with poly(ethylene glycol) (PEG).[61]

Polyol method. The polyol method is similar to a sol–gel process. It is based on the alkaline hydrolysis of Fe^{2+} and Fe^{3+} salts in a stoichiometric mixture of polyols (*e.g.* diethylene glycol (DEG) and *N*-methyldiethanolamine (NMDA)). The liquid polyol acts as the solvent of the metallic precursor. Polyols also serve as reducing agents and stabilizers allowing the possibility to control the size and shape of the obtained materials and preventing interparticle aggregation. The variation of temperature, nature of precursors, the choice of the solvents and the duration of the reaction influence the size

and structure of the resulting magnetic nanoparticles.[23] The relaxation properties of particles prepared this way could be of great relevance for biosensor applications.[12]

In this method, the surface of the nanoparticle is directly coated by hydrophilic polyol ligands allowing an easy dispersion in aqueous media and other polar solvents. In addition, the relatively high reaction temperature favours particles with a higher crystallinity and therefore a higher magnetization. Ultimately, the size distribution of the nanoparticles is much narrower than those particles produced by traditional methods[30] but wider than those prepared by thermal decomposition of organometallic compounds.

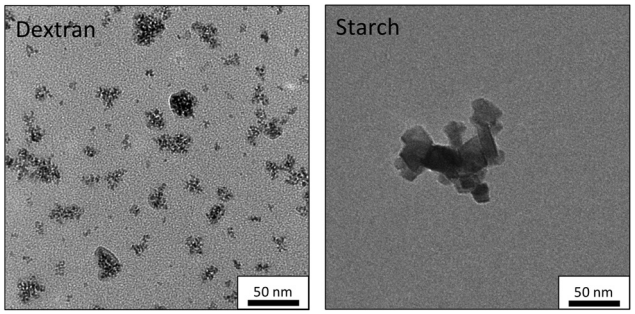

Fig. 4 TEM pictures showing multi-core particles prepared from aqueous phase synthesis of iron oxide cores obtained using dextran (left) and starch (right) coatings.

Multi-core nanoparticles

Most methods of synthesis and coating of magnetic nanoparticles yield multi-core entities, and multi-core particles are far more common than single-core particles. As with single-core nanoparticles, the synthesis methods may be classified according to whether the processing phase is aqueous or organic, although a third phase is also possible, *viz.* the gaseous phase, as used in laser pyrolysis.

Some aspects of the multi-core particles' internal structure may also be related to the way in which the cores come together. Most commonly this happens at the initial nucleation and growth stage, as the cores tend to aggregate immediately after their formation. Coating of these primary aggregates then leads to the multi-core nanoparticles. Less commonly, multi-core nanoparticles with a controlled microstructure may be prepared by incorporating single-core nanoparticles into organic templates such as liposomes or engineered vesicles.

For this reason, the roles of different coating methods are discussed below, as part of the descriptions of the influence of the three different synthesis phases that are used.

Multi-core nanoparticles from aqueous phase synthesis

Most of the multi-core magnetic nanoparticles synthesized in aqueous phases are produced by methods based on the Massart procedure,[33] as described in the single-core synthesis section. For example, iron oxide nanoparticles have been prepared by basic precipitation followed by acidification with nitric acid.[62] Although these particles were used for the adsorption of negatively charged ligands, the same procedure could also be used for further modification, *e.g.* silanisation and PEGylation to obtain multi-core particles.

Alternative synthesis routes have been developed by precipitation of $FeSO_4$ in the presence of NaOH and a mild oxidant (KNO_3), with subsequent aging. Although this method produces nanoparticles up to 200 nm size, by adjusting the $FeSO_4$ concentration and the solvent, iron oxide particles with diameters down to 30 nm and different shapes (spherical, cubic or octahedral) were obtained.[63] The role of the initial molar ratios of Fe^{2+}/NO_3^- and Fe^{2+}/OH^- in a $FeCl_2$–$NaNO_3$–NaOH aqueous system on the size, morphology and magnetothermal capacity of the resulting multi-core particles have also been evaluated.[64] Also the sequence of adding $NaNO_3$ to NaOH and Fe^{2+} was found to have a significant influence on the nanoparticles properties.[64]

The greatest variety in aqueous syntheses relates to the coatings of the cores, rather than the cores themselves. Indeed, coatings play a pivotal role in aqueous-phase multi-core syntheses, both in terms of establishing the final structure and magnetic character of the nanoparticles, and also their biocompatibility and biodistribution in the human body. The most commonly used coatings and the multi-core nanoparticles they produce are discussed below.

Polysaccharide coatings. Multi-core particles can be obtained by using a polysaccharide coating to encapsulate the aggregates containing several magnetic cores (Fig. 4). Examples of such particles include the magnetic resonance imaging (MRI) contrast agents Endorem® (no longer commercially available) and Resovist® (Fujifilm RI Pharma, Japan), both of which comprise 4 to 8 nm cores. These cores are coated with dextran or carboxydextran, respectively, to make particles with mean hydrodynamic sizes of 150 and 60 nm, respectively.[65] The synthesis of differently sized starch coated nanoparticles to be used as MRI contrast agents has also been described.[66] For preclinical applications, *e.g.* small animal MRI, carboxydextran coated, differently sized iron oxide nanoparticles of pharmaceutical quality are available (FeraSpin™ R and FeraSpin™ XS to XXL, nanoPET Pharma GmbH, Germany).

Multi-core particles for hyperthermia cancer treatment have been prepared by applying a high pressure homogenization process during the iron oxide precipitation, resulting in BNF (Bionized NanoFerrite) particles. This synthesis produces individual crystals with mean diameters of 15–20 nm, and then creates aggregates to form a multi-core particle.[67] The aggregates are then coated with dextran or starch, and the final particles possess a hydrodynamic diameter of about 100 nm (Fig. 4). These particles may be useful for hyperthermia cancer treatment as they provide high heating rates at magnetic field strengths >30 kA m^{-1}.[68–72]

Molecular coating. Iron oxide nanoparticle clusters can also be coated with various molecules to maintain the colloidal stability *via* electrostatic repulsion. The most commonly used

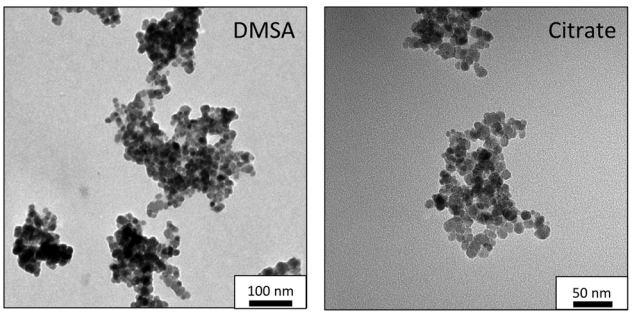

Fig. 5 TEM picture showing multi-core particles prepared from aqueous phase synthesis of iron oxide cores coated with citrate (right) and DMSA (left, prepared following the protocol described by Luengo *et al.*[76]).

chemical in this context is citric acid.[73] An example of multi-core particles coated with citrate, under research and development at nanoPET Pharma GmbH, is shown in Fig. 5. Other molecular coating materials which can be used for stabilisation include tartaric acid,[74] gluconic acid[75] or dimercaptosuccinic acid[76] (Fig. 5). In contrast to steric stabilisation *via* polymers, the colloidal stability of these coated particles strongly depends on the protonation/deprotonation of the coating molecules, and thus on the pH as well as on the ionic strength of the suspension medium.

Hydrophilic polymer coating. Iron oxide nanoparticles of around 6 nm have been clustered by hydrophilic polymers such as poly(trimethylammonium ethylacrylate methyl sulfate)-*b*-poly(acrylamide) (PTEA-*b*-PAM). Multi-core particles are obtained by mixing a solution containing the particles with another solution containing the polymer at the same concentration and pH. This procedure leads to multi-core particles containing between tens and hundreds of cores and a hydrodynamic diameter in the range of 70–150 nm.[77] The relaxivities of these materials indicate a better performance as MRI contrast agents than their single-core counterparts.[77]

Liposomes, lipid or polymeric vesicles encapsulation. Magnetic nanoparticles have been encapsulated in liposomes of around 200 nm formed by egg phosphatidylcholine (EPC) and distearoyl-SN-glycero-3-phosphoethanolamine-*N*-[methoxy-(poly(ethyleneglycol))-2000].[78] Nanoparticles have also been encapsulated within the membrane of poly(trimethylene carbonate)-*b*-poly(L-glutamic acid) (PTMC-*b*-PGA) block copolymer vesicles with sizes in the range of 100–400 nm.[79] In this case, the vesicles were also loaded with doxorubicin for drug delivery.

Multi-core nanoparticles from organic phase synthesis

Thermal decomposition of organometallic compounds. Single-core iron oxide nanoparticles obtained by thermal decomposition of organometallic compounds,[48] prepared as described above, have been clustered by several methods to improve their physicochemical properties especially for their use on hyperthermia treatments or as MRI contrast agents. Some examples are listed below.

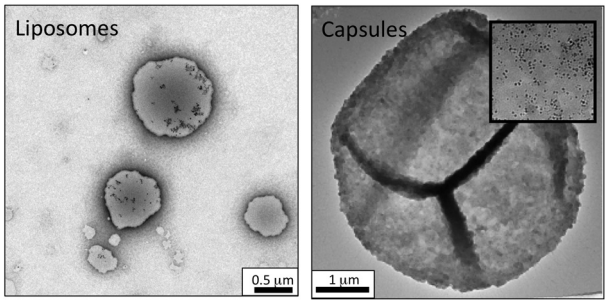

Fig. 6 (Left) TEM picture showing liposomes containing several magnetic cores obtained by thermal decomposition in organic media, (unpublished work). (Right) TEM picture showing multi-core capsules, where the magnetic cores are forming a part of the capsule surface (Inset). Image modified from Abbasi *et al.*[85] Reprinted with permission from {*J. Phys. Chem. C*, 2011, **115**(14), 6257–6264}. Copyright 2011 American Chemical Society.

Polysaccharide coatings. Encapsulation of magnetic nanoparticles in a shell of DOPA (3,4-dihydroxyphenylalanine)-conjugated chitosan oligosaccharide[80] has led to particles with a hydrodynamic diameter of around 150 nm that contain several 30 nm iron oxide cores inside. This approach combines the colloidal stability of chitosan with the strong affinity of DOPA to the iron oxide surface, also resulting in very stable particles with interesting potential as hyperthermia agents.[80]

Silica coating. Silica-coated multi-core particles of around 150–300 nm have been obtained by combining sol–gel chemistry and supercritical fluid technology, using cores that where prepared by thermal decomposition of iron pentacarbonyl ($Fe(CO)_5$) in the presence of oleic acid.[81] These materials have been proposed as T2 MRI contrast agents.

Liposomes, lipid or polymeric vesicle encapsulation. Iron oxide nanoparticles have been clustered by amphiphilic polymers in micelles (Fig. 6) to increase their relaxivity for use as MRI contrast agents. Magnetic nanoparticles have been encapsulated inside the hydrophobic core of a polymeric micelle formed by an amphiphilic diblock copolymer of PCL-*b*-PEG (poly(ε-caprolactone)-*b*-poly(ethyleneglycol)) whose surface was stabilized by a PEG shell, that improves their stability in water.[82] The effect of the multi-core particle size using mPEG-PLA (methoxy poly(ethylene glycol)-poly(lactide)) micelles have also been studied. In the latter case, increasing the amount of copolymer/particles ratio led to a decrease in the final cluster sizes, which affected the relaxivity properties of the multi-core particles.[83]

Amphiphilic block copolymers have been used to produce multi-core particles whose cores were prepared in organic solvents. An anticancer drug was simultaneously encapsulated with the cores, to be used for drug delivery.[84]

Magnetic nanoparticles have also been embedded into the walls of polyelectrolyte multilayer capsules of around 4 μm.[85] These multi-core nanoparticles display a controlled microstructure providing a good opportunity to study the effect of the geometric distribution on the magnetic properties of these systems (Fig. 6).

Polyol method. Based on the polyol route, using a DEG/NMDA mixture, citrate coated multi-core flower-shaped maghemite structures, consisting of smaller grains between 11 and 30 nm have been prepared.[86,87] The close contact of the cores in these multi-core flower-shaped structures allows exchange coupling among the cores enhancing their magnetic properties in comparison to single-core counterparts or matrix-embedded clusters, in which the magnetic cores present dipole–dipole interactions. As a result, improved heating parameters for magnetic hyperthermia and longitudinal and transverse relaxivities for MRI contrast generation have been reported.

Multi-core nanoparticles from gas phase synthesis

Iron oxide nanoparticles have been reproducibly produced in the gaseous phase using laser pyrolysis.[88,89] In general terms, this procedure generates the nanoparticles by means of the laser heating of vapors of an organometallic precursor in a vacuum chamber at reduced pressure. The nanoparticles present in the gas stream that exit the chamber are collected on a filter downstream. This procedure has the advantage of generating the nanoparticles with high homogeneity, in continuous form.

For the case of iron oxide nanoparticles the precursor is iron pentacarbonyl and the carrier gas (that also absorbs the CO_2 laser energy to heat the mixture) is ethylene. The reactant gas is confined to the flow axis by a sheath flow of argon to minimize particle deposition on the reactor walls. A second argon flux, used to avoid the deposition of powder on the laser windows, carries the air needed to produce the *in situ* oxidation of the iron nanoparticles initially formed.

The main parameters that affect the particle synthesis are the ethylene flux, the evaporation temperature of the precursor and the laser power. The particle sizes commonly obtained for iron oxides are in the range of 2–5 nm depending on the process conditions with average productivities of 20 mg h^{-1}.

The powders obtained can be dispersed in water by means of extensive sonication. They have also been simultaneously coated by dextran, resulting in multi-core particles with hydrodynamic sizes below 50 nm, able to be employed as contrast agents for MRI for research purposes.[90]

Summary and outlook

In this work we have reviewed current perspectives on the synthesis of single-core and multi-core magnetic iron oxide nanoparticles for biomedical applications. There are more examples of multi-core magnetic particles than single-core ones, especially since coating of particle aggregates within a matrix will result in multi-core particles. However, it is difficult to control the number of cores, inter-core distances and spatial distribution when generating multi-core particles.

Many parameters of the synthesis procedure may have a strong effect on the particles obtained, including temperature, reagent concentrations, surfactant concentrations, and stirring conditions. This is one of the reasons why scaling-up of some of these synthesis routes is extremely complicated. Indeed, one of the difficulties that particle synthesis faces is in batch-to-batch reproducibility. This has led to recent work on alternative reaction platforms that can offer more consistent results. One such platform is the use of microwave irradiation as a heating source.[91,92] Modern microwave reactors specifically designed for chemical synthesis provide good temperature and pressure control inside the reaction vessel, resulting in a careful control of the reaction conditions and therefore good reproducibility,[93] while also significantly reducing reaction times. These advantages open the way for new biomedical applications that require short times between particle synthesis and application, such as the generation of dual PET (Positron Emission Tomography)/MRI nanoparticles[94] using isotopes with short half-life.

As mentioned in the introduction, the magnetic properties of the nanoparticles may change significantly depending on their aggregation degree (and further agglomeration), which depends on a large extent to the synthesis method. It is important to bear in mind that, given the completely different environment of the particles when *in vivo*, their magnetic properties may be significantly altered once in the blood stream, or in the different tissues. The complex biological matrices may lead to nanoparticle agglomeration,[95] having strong effects on the their performance.[96]

Unravelling the parameters that affect the magnetic properties of single- and multi-core particles, and understanding their implications on biomedical applications, is an on-going endeavour for the scientific community. To achieve this end, and be able to produce robust materials, reliable synthesis methods able to reproduce nanoparticle size, shape and structural homogeneity are required. We hope that by regularly reviewing the progress that is being made, it will be possible to more quickly reach the desired standard. When reached, that will be a major achievement, and one of great relevance to the standardisation – and therefore acceptance and adoption – of any number of possible diagnostic and therapeutic applications of magnetic nanoparticles.

Acknowledgements

This work was supported by the European Commission Framework Programme 7 under grant agreement no [604448], Nanomag project. LG is the beneficiary of a post-doctoral grant from the AXA Research Fund.

Notes and references

1 M. Colombo, S. Carregal-Romero, M. F. Casula, L. Gutiérrez, M. P. Morales, I. B. Böhm, J. T. Heverhagen, D. Prosperi and W. J. Parak, *Chem. Soc. Rev.*, 2012, **41**, 4306–4334.

2 Q. A. Pankhurst, N. T. K. Thanh, S. K. Jones and J. Dobson, *J. Phys. D: Appl. Phys.*, 2009, **42**, 224001.
3 T. Z. G. de la Torre, A. Mezger, D. Herthnek, C. Johansson, P. Svedlindh, M. Nilsson and M. Strømme, *Biosens. Bioelectron.*, 2011, **29**, 195–199.
4 A. Jordan, R. Scholz, P. Wust, H. Fähling and R. Felix, *J. Magn. Magn. Mater.*, 1999, **201**, 413–419.
5 A. Ranzoni, G. Sabatte, L. J. van Ijzendoorn and M. W. J. Prins, *ACS Nano*, 2012, **6**, 3134–3141.
6 R. Mejías, S. Pérez-Yagüe, L. Gutiérrez, L. I. Cabrera, R. Spada, P. Acedo, C. J. Serna, F. J. Lázaro, T. Villanueva, M. D. P. Morales and D. F. Barber, *Biomaterials*, 2011, **32**, 2938–2952.
7 J. Zou, W. Zhang, D. Poe, J. Qin, A. Fornara, Y. Zhang, U. A. Ramadan, M. Muhammed and I. Pyykkö, *Nanomedicine*, 2010, **5**, 739–754.
8 D. Eberbeck, C. L. Dennis, N. F. Huls, K. L. Krycka, C. Gruttner and F. Westphal, *IEEE Trans. Magn.*, 2013, **49**, 269–274.
9 R. M. Ferguson, A. P. Khandhar and K. M. Krishnan, *J. Appl. Phys.*, 2012, **111**, 07B318.
10 C. F. Teixeira, E. Neuhauss, R. Ben, J. Romanzini and C. Graeff-Teixeira, *PLoS Neglected Trop. Dis.*, 2007, **1**, e73.
11 S. Karl, L. Gutiérrez, R. Lucyk-Maurer, R. Kerr, R. R. F. Candido, S. Q. Toh, M. Saunders, J. A. Shaw, A. Suvorova, A. Hofmann, M. J. House, R. C. Woodward, C. Graeff-Teixera, T. G. St. Pierre and M. K. Jones, *PLoS Neglected Trop. Dis.*, 2013, **7**, e2219.
12 A. Fornara, P. Johansson, K. Petersson, S. Gustafsson, J. Qin, E. Olsson, D. Ilver, A. Krozer, M. Muhammed and C. Johansson, *Nano Lett.*, 2008, **8**, 3423–3428.
13 A. Meddahi-Pellé, A. Legrand, A. Marcellan, L. Louedec, D. Letourneur and L. Leibler, *Angew. Chem., Int. Ed.*, 2014, **53**, 6369–6373.
14 N. Gehrke, A. Briel, F. Ludwig, H. Remmer, T. Wawrzik and S. Wellert, in *Magnetic Particle Imaging*, ed. T. M. Buzug and J. Borgert, Springer, Berlin, Heidelberg, 2012, vol. 140, ch. 16, pp. 99–103.
15 Y. Min, M. Akbulut, K. Kristiansen, Y. Golan and J. Israelachvili, *Nat. Mater.*, 2008, **7**, 527–538.
16 K. J. Bishop, C. E. Wilmer, S. Soh and B. A. Grzybowski, *Small*, 2009, **5**, 1600–1630.
17 L. Gutierrez, M. P. Morales and F. J. Lazaro, *Phys. Chem. Chem. Phys.*, 2014, 4456–4464.
18 X. Batlle and A. Labarta, *J. Phys. D: Appl. Phys.*, 2002, **35**, R15.
19 S. Dutz, J. H. Clement, D. Eberbeck, T. Gelbrich, R. Hergt, R. Müller, J. Wotschadlo and M. Zeisberger, *J. Magn. Magn. Mater.*, 2009, **321**, 1501–1504.
20 S. Dutz, M. Kettering, I. Hilger, R. Müller and M. Zeisberger, *Nanotechnology*, 2011, **22**, 265102.
21 B. Mehdaoui, R. P. Tan, A. Meffre, J. Carrey, S. Lachaize, B. Chaudret and M. Respaud, *Phys. Rev. B: Condens. Matter*, 2013, **87**, 174419.
22 I. Hilger and W. A. Kaiser, *Nanomedicine*, 2012, **7**, 1443–1459.
23 S. Gustafsson, A. Fornara, K. Petersson, C. Johansson, M. Muhammed and E. Olsson, *Cryst. Growth Des.*, 2010, **10**, 2278–2284.
24 L. Gutiérrez, F. J. Lázaro, A. R. Abadía, M. S. Romero, C. Quintana, M. Puerto Morales, C. Patiño and R. Arranz, *J. Inorg. Biochem.*, 2006, **100**, 1790–1799.
25 L. Gutiérrez, R. Mejías, D. F. Barber, S. Veintemillas-Verdaguer, C. J. Serna, F. J. Lázaro and M. P. Morales, *J. Phys. D: Appl. Phys.*, 2011, **44**, 255002.
26 A. López, L. Gutiérrez and F. J. Lázaro, *Phys. Med. Biol.*, 2007, **52**, 5043–5056.
27 C. A. Gorski and M. M. Scherer, *Am. Mineral.*, 2010, **95**, 1017–1026.
28 M. Calero, L. Gutiérrez, G. Salas, Y. Luengo, A. Lázaro, P. Acedo, M. P. Morales, R. Miranda and A. Villanueva, *Nanomedicine*, 2014, **10**, 733–743.
29 C. Grüttner, K. Müller, J. Teller and F. Westphal, *Int. J. Hyperthermia*, 2013, **29**, 777–789.
30 S. Laurent, D. Forge, M. Port, A. Roch, C. Robic, L. Vander Elst and R. N. Muller, *Chem. Rev.*, 2008, **108**, 2064–2110.
31 V. R. Dayeh, S. L. Chow, K. Schirmer, D. H. Lynn and N. C. Bols, *Ecotoxicol. Environ. Saf.*, 2004, **57**, 375–382.
32 K.-i. Kusumoto and T. Ishikawa, *J. Controlled Release*, 2010, **147**, 246–252.
33 R. Massart, *IEEE Trans. Magn.*, 1981, **17**, 1247–1248.
34 M. Taupitz, J. Schnorr, C. Abramjuk, S. Wagner, H. Pilgrimm, H. Hünigen and B. Hamm, *J. Magn. Reson.*, 2000, **12**, 905–911.
35 H. Pilgrimm, *U.S. Patent* No. 6,638,494. Washington, DC, U.S. Patent and Trademark Office., 2003.
36 S. Wagner, J. Schnorr, H. Pilgrimm, B. Hamm and M. Taupitz, *Invest. Radiol.*, 2002, **37**, 167–177.
37 J. r. Schnorr, S. Wagner, C. Abramjuk, R. Drees, T. Schink, E. A. Schellenberger, H. Pilgrimm, B. Hamm and M. Taupitz, *Radiology*, 2006, **240**, 90–100.
38 J. Schnorr, S. Wagner, C. Abramjuk, I. Wojner, T. Schink, T. J. Kroencke, E. Schellenberger, B. Hamm, H. Pilgrimm and M. Taupitz, *Invest. Radiol.*, 2004, **39**, 546–553.
39 M. Taupitz, S. Wagner, J. Schnorr, I. Kravec, H. Pilgrimm, H. Bergmann-Fritsch and B. Hamm, *Invest. Radiol.*, 2004, **39**, 394–405.
40 B. Chanteau, J. Fresnais and J. F. Berret, *Langmuir*, 2009, **25**, 9064–9070.
41 Q. L. Vuong, J.-F. Berret, J. Fresnais, Y. Gossuin and O. Sandre, *Adv. Healthcare Mater.*, 2012, **1**, 502–512.
42 W. Stöber, A. Fink and E. Bohn, *J. Colloid Interface Sci.*, 1968, **26**, 62–69.
43 S. Santra, R. Tapec, N. Theodoropoulou, J. Dobson, A. Hebard and W. Tan, *Langmuir*, 2001, **17**, 2900–2906.
44 P. Tartaj and C. J. Serna, *Chem. Mater.*, 2002, **14**, 4396–4402.
45 A. P. Philipse, M. P. B. van Bruggen and C. Pathmamanoharan, *Langmuir*, 1994, **10**, 92–99.
46 S. L. C. Pinho, G. A. Pereira, P. Voisin, J. Kassem, V. Bouchaud, L. Etienne, J. A. Peters, L. Carlos, S. Mornet,

C. F. G. C. Geraldes, J. Rocha and M.-H. Delville, *ACS Nano*, 2010, **4**, 5339–5349.
47 T. Hyeon, S. S. Lee, J. Park, Y. Chung and H. B. Na, *J. Am. Chem. Soc.*, 2001, **123**, 12798–12801.
48 D. Kim, N. Lee, M. Park, B. H. Kim, K. An and T. Hyeon, *J. Am. Chem. Soc.*, 2009, **131**, 454–455.
49 A. G. Roca, M. P. Morales, K. O'Grady and C. J. Serna, *Nanotechnology*, 2006, **17**, 2783.
50 A. G. Roca, J. F. Marco, M. d. P. Morales and C. J. Serna, *J. Phys. Chem. C*, 2007, **111**, 18577–18584.
51 J. Park, E. Lee, N.-M. Hwang, M. Kang, S. C. Kim, Y. Hwang, J.-G. Park, H.-J. Noh, J.-Y. Kim, J.-H. Park and T. Hyeon, *Angew. Chem., Int. Ed.*, 2005, **44**, 2872–2877.
52 W. Baaziz, B. P. Pichon, S. Fleutot, Y. Liu, C. Lefevre, J.-M. Greneche, M. Toumi, T. Mhiri and S. Begin-Colin, *J. Phys. Chem. C*, 2014, **118**, 3795–3810.
53 E. Wetterskog, M. Agthe, A. Mayence, J. Grins, D. Wang, S. Rana, A. Ahniyaz, G. Salazar-Alvarez and L. Bergström, *Sci. Technol. Adv. Mater.*, 2014, **15**, 055010.
54 G. Salas, C. Casado, F. J. Teran, R. Miranda, C. J. Serna and M. P. Morales, *J. Mater. Chem.*, 2012, **22**, 21065–21075.
55 E. S. Jang, *J. Korean Chem. Soc.*, 2012, **56**, 478–483.
56 C. Vogt, M. S. Toprak, M. Muhammed, S. Laurent, J.-L. Bridot and R. Müller, *J. Nanopart. Res.*, 2010, **12**, 1137–1147.
57 M. Zhang, B. L. Cushing and C. J. O. Connor, *Nanotechnology*, 2008, **19**, 085601.
58 F. Ye, S. Laurent, A. Fornara, L. Astolfi, J. Qin, A. Roch, A. Martini, M. S. Toprak, R. N. Muller and M. Muhammed, *Contrast Media Mol. Imaging*, 2012, **7**, 460–468.
59 D. C. Lee, F. V. Mikulec, J. M. Pelaez, B. Koo and B. A. Korgel, *J. Phys. Chem. B*, 2006, **110**, 11160–11166.
60 T. Pellegrino, L. Manna, S. Kudera, T. Liedl, D. Koktysh, A. L. Rogach, S. Keller, J. Rädler, G. Natile and W. J. Parak, *Nano Lett.*, 2004, **4**, 703–707.
61 W. W. Yu, E. Chang, C. M. Sayes, R. Drezek and V. L. Colvin, *Nanotechnology*, 2006, **17**, 4483.
62 N. Fauconnier, A. Bée, J. Roger and J. N. Pons, *J. Mol. Liq.*, 1999, **83**, 233–242.
63 M. A. Verges, R. Costo, A. G. Roca, J. F. Marco, G. F. Goya, C. J. Serna and M. P. Morales, *J. Phys. D: Appl. Phys.*, 2008, **41**, 134003–134013.
64 Z. Li, M. Kawashita, N. Araki, M. Mitsumori, M. Hiraoka and M. Doi, *J. Biomater. Appl.*, 2011, **25**, 643–661.
65 C. W. Jung and P. Jacobs, *Magn. Reson. Imaging*, 1995, **13**, 661–674.
66 D. K. Kim, M. Mikhaylova, F. H. Wang, J. Kehr, B. Bjelke, Y. Zhang, T. Tsakalakos and M. Muhammed, *Chem. Mater.*, 2003, **15**, 4343–4351.
67 C. Grüttner, K. Müller, J. Teller, F. Westphal, A. R. Foreman and R. Ivkov, *J. Magn. Magn. Mater.*, 2007, **311**, 181–186.
68 D. E. Bordelon, C. Cornejo, C. Grüttner, F. Westphal, T. L. DeWeese and R. Ivkov, *J. Appl. Phys.*, 2011, **109**, 124904.
69 C. L. Dennis, A. J. Jackson, J. A. Borchers, P. J. Hoopes, R. Strawbridge, A. R. Foreman, J. van Lierop, C. Grüttner and R. Ivkov, *Nanotechnology*, 2009, **20**, 395103–395110.
70 C. L. Dennis, A. J. Jackson, J. A. Borchers, R. Ivkov, A. R. Foreman, J. W. Lau, E. Görnitz and C. Grüttner, *J. Appl. Phys.*, 2008, **103**, 07A319.
71 P. J. Hoopes, J. A. Tate, J. A. Ogden, R. Strawbridge, S. N. Fiering, A. A. Petryk, S. M. Cassim, A. J. Giustini, E. Demidenko, R. Ivkov, S. Barry, P. Chinn and A. Foreman, *Proc. SPIE*, 2009, **7181**, 71810P–71811P.
72 K. L. Krycka, A. J. Jackson, J. A. Borchers, J. Shih, R. Briber, R. Ivkov, C. Grüttner and C. L. Dennis, *J. Appl. Phys.*, 2011, **109**, 07B513.
73 L. Li, K. Y. Mak, C. W. Leung, K. Y. Chan, W. K. Chan, W. Zhong and P. W. T. Pong, *Microelectron. Eng.*, 2013, **110**, 329–334.
74 J. Yan, S. Mo, J. Nie, W. Chen, X. Shen, J. Hu, G. Hao and H. Tong, *Colloids Surf., A*, 2009, **340**, 109–114.
75 N. Fauconnier, A. Bee, J. Roger and J. N. Pons, in *Trends in Colloid and Interface Science X*, ed. C. Solans, M. R. Infante and M. J. García-Celma, Steinkopff, 1996, vol. 100, ch. 42, pp. 212–216.
76 Y. Luengo, S. Nardecchia, M. P. Morales and M. C. Serrano, *Nanoscale*, 2013, **5**, 11428–11437.
77 J.-F. Berret, N. Schonbeck, F. Gazeau, D. El Kharrat, O. Sandre, A. Vacher and M. Airiau, *J. Am. Chem. Soc.*, 2006, **128**, 1755–1761.
78 M.-S. Martina, J.-P. Fortin, C. Ménager, O. Clément, G. Barratt, C. Grabielle-Madelmont, F. Gazeau, V. Cabuil and S. Lesieur, *J. Am. Chem. Soc.*, 2005, **127**, 10676–10685.
79 C. Sanson, O. Diou, J. Thévenot, E. Ibarboure, A. Soum, A. Brûlet, S. Miraux, E. Thiaudière, S. Tan, A. Brisson, V. Dupuis, O. Sandre and S. Lecommandoux, *ACS Nano*, 2011, **5**, 1122–1140.
80 K. H. Bae, M. Park, M. J. Do, N. Lee, J. H. Ryu, G. W. Kim, C. Kim, T. G. Park and T. Hyeon, *ACS Nano*, 2012, **6**, 5266–5273.
81 E. Taboada, R. Solanas, E. Rodriguez, R. Weissleder and A. Roig, *Adv. Funct. Mater.*, 2009, **19**, 2319–2324.
82 H. Ai, C. Flask, B. Weinberg, X. T. Shuai, M. D. Pagel, D. Farrell, J. Duerk and J. Gao, *Adv. Mater.*, 2005, **17**, 1949–1952.
83 X. Xie and C. Zhang, *J. Nanomater.*, 2011, **2011**, 152524.
84 J. Yang, C.-H. Lee, H.-J. Ko, J.-S. Suh, H.-G. Yoon, K. Lee, Y.-M. Huh and S. Haam, *Angew. Chem., Int. Ed.*, 2007, **46**, 8836–8839.
85 A. Z. Abbasi, L. Gutiérrez, L. L. Del Mercato, F. Herranz, O. Chubykalo-Fesenko, S. Veintemillas-Verdaguer, W. J. Parak, M. P. Morales, J. M. González, A. Hernando and P. De La Presa, *J. Phys. Chem. C*, 2011, **115**, 6257–6264.
86 P. Hugounenq, M. Levy, D. Alloyeau, L. Lartigue, E. Dubois, V. Cabuil, C. Ricolleau, S. Roux, C. Wilhelm, F. Gazeau and R. Bazzi, *J. Phys. Chem. C*, 2012, **116**, 15702–15712.
87 L. Lartigue, P. Hugounenq, D. Alloyeou, S. P. Clarke, M. Levy, J. C. Bacri, R. Bazzi, D. F. Brougham, C. Wilhelm and F. Gazeau, *ACS Nano*, 2012, **6**, 10935–10949.

88 R. Alexandrescu, V. Bouzas, R. Costo, F. Dumitrache, M. A. García, M. P. Morales, I. Morjan, C. J. Serna and S. Veintemillas-Verdaguer, *AIP Conf. Proc.*, 2010, **1275**, 30–32.
89 S. Veintemillas-Verdaguer, M. P. Morales and C. J. Serna, *Mater. Lett.*, 1998, **35**, 227–231.
90 S. Veintemillas-Verdaguer, M. d. P. Morales, O. Bomati-Miguel, C. Bautista, X. Zhao, P. Bonville, R. P. d. Alejo, J. Ruiz-Cabello, M. Santos, F. J. Tendillo-Cortijo and J. Ferreirós, *J. Phys. D: Appl. Phys.*, 2004, **37**, 2054.
91 F. Y. Jiang, C. M. Wang, Y. Fu and R. C. Liu, *J. Alloys Compd.*, 2010, **503**, L31–L33.
92 J. G. Parsons, C. Luna, C. E. Botez, J. Elizalde and J. L. Gardea-Torresdey, *J. Phys. Chem. Solids*, 2009, **70**, 555–560.
93 M. Baghbanzadeh, L. Carbone, P. D. Cozzoli and C. O. Kappe, *Angew. Chem., Int. Ed.*, 2011, **50**, 11312–11359.
94 R. M. Wong, D. A. Gilbert, K. Liu and A. Y. Louie, *ACS Nano*, 2012, **6**, 3461–3467.
95 H. T. R. Wiogo, M. Lim, V. Bulmus, L. Gutiérrez, R. C. Woodward and R. Amal, *Langmuir*, 2012, **28**, 4346–4356.
96 M. L. Etheridge, K. R. Hurley, J. Zhang, S. Jeon, H. L. Ring, C. Hogan, C. L. Haynes, M. Garwood and J. C. Bischof, *Technology*, 2014, **02**, 214–228.

